ions, indicating that the rate of dissociation, $K_d = 1/\tau$ (*15*), of the conducting dimer is greatly increased by the presence of the CH_3 moiety. The magnitude of this reduction in channel stability, which corresponds to approximately 2.4 kcal/mole independently of the type of cation present in the channel, is consistent with the expected decrease of the energy of dimerization due to the presence of the bulky CH_3 moiety. When all six intermolecular hydrogen bonds are formed in the head-to-head dimerization of *N*-acetyl-G, there results a methyl-methyl steric crowding of several kilocalories per mole [see figure 14 in (*17*)]. This crowding could be relieved by shifting from six to four hydrogen bonds with water from the channel partially satisfying the two broken hydrogen bonds. The four hydrogen-bonded dimer, however, would not as adequately provide for lowering of the permeation barrier for an ion passing the junction between two molecules, and the conductance would decrease. Thus an oscillation between head-to-head dimeric structures of six and of four intermolecular hydrogen bonds would provide an explanation for the fluctuating conductance of a single *N*-acetyl-G channel. With respect to the double-stranded structures, it is particularly difficult to rationalize why they would be so stable with lifetimes measured in hours or days in polar organic solvents and yet have lifetimes of the order of tens of milliseconds within the less polar lipid membrane. However, the behavior of the *N*-acetyl-G derivative is predictable in terms of the conductive species being a head-to-head dimer.

The results obtained here for *N*-acetyl gramicidin, therefore, further support the head-to-head dimer structure for the ion-conducting channel. In general, any modification of the amino terminus—for example, *N*-pyromellitylization, *N*-succinylation, *N*-malonyl dimerization, or even this subtle substitution of methyl moiety for a hydrogen—causes dramatic and predictable changes in the channel properties, whereas similar derivatives made at the carboxy terminus causes relatively small but also predictable effects on the channel properties when the channel is considered in terms of the head-to-head dimer.

GABOR SZABO
Department of Physiology and Biophysics, University of Texas Medical Branch, Galveston 77550
DAN W. URRY
Laboratory of Molecular Biophysics and *Cardiovascular Research and Training Center, University of Alabama Medical Center, Birmingham 35294*

References and Notes

1. B. Hille, *Biophys. J.* **22**, 283 (1978).
2. G. Eisenman, J. Sandblom, E. Neher, *ibid.*, p. 307.
3. S. B. Hladky and D. A. Haydon, *Biochim. Biophys. Acta* **274**, 294 (1972).
4. M. D. Goodall, *ibid.* **219**, 471 (1970); E. Bamberg and P. Läuger, *J. Membr. Biol.* **11**, 177 (1973); H. A. Kolb, P. Läuger, E. Bamberg, *ibid.* **20**, 133 (1975).
5. D. W. Urry, *Proc. Natl. Acad. Sci. U.S.A.* **68**, 672 (1971).
6. ———, M. C. Goodall, J. D. Glickson, D. F. Mayers, *ibid.*, p. 1907.
7. D. W. Urry, *ibid.* **69**, 1610 (1972); in *Conformation of Biological Molecules and Polymers, The Jerusalem Symposia on Quantum Chemistry and Biochemistry*, B. Pullman and E. D. Bergmann, Eds. (Israel Academy of Sciences and Humanities, Jerusalem, 1973), vol. 5, pp. 723–736 (1973); ———, M. M. Long, M. Jacobs, R. D. Harris, *Ann. N.Y. Acad. Sci.* **264**, 203 (1975).
8. W. R. Veatch, E. T. Fossel, E. R. Biout, *Biochemistry* **13**, 5249 (1974).
9. W. R. Veatch and E. R. Blout, *ibid.*, p. 5257.
10. E. T. Fossel, W. R. Veatch, Y. A. Ovchinnikov, E. R. Blout, *ibid.*, p. 5264.
11. E. Bamberg and K. Janko, *Biochim. Biophys. Acta* **465**, 486 (1977).
12. E. Bamberg, H. J. Apell, H. Alpes, *Proc. Natl. Acad. Sci. U.S.A.* **74**, 2402 (1977); H. J. Apell, E. Bamberg, H. Alpes, P. Läuger, *J. Membr. Biol.* **31**, 171 (1977).
13. R. J. Bradley, D. W. Urry, K. Okamoto, R. S. Rapaka, *Science* **200**, 435 (1978).
14. M. C. Goodall, *Arch. Biochem. Biophys.* **147**, 129 (1971).
15. H. A. Kolb and E. Bamberg, *Biochim. Biophys. Acta* **464**, 127 (1977).
16. E. Neher and B. Sakman, *Nature (London)* **260**, 799 (1976).
17. D. W. Urry, *Biochim. Biophys. Acta* **265**, 115 (1972).
18. G. Szabo, G. Eisenman, S. Ciani, *J. Membr. Biol.* **1**, 346 (1969).

19. Supported by PHS grants NS-13778, HL-19639, and HL-11310. We thank Mark Wiederspahn for technical assistance.

29 June 1978; revised 26 September 1978

Irradiance Modulation Used to Examine Sound-Radiating Cuticular Motion in Insects

Abstract. *A new, noncontact, optical technique for measurement of movements smaller than a few micrometers has been used to record cuticular motion of insects as they produce sound. The instrument described is highly sensitive to surface movement and offers good spatial resolution, broad dynamic range, tolerance of substantial background motion of the target surface, portability, and simplicity, and as such appears to hold promise for measuring other biologically interesting motions that have proved difficult to measure by other available techniques.*

In animals, production and reception of mechanical vibration constitutes a principal mode of communication and means of monitoring the environment. The development of hearing mechanisms throughout the animal kingdom attests to the importance of the airborne vibration we call sound. But production or reception of any type of vibration involves the motion, usually at minute amplitudes, of body surfaces. This surface motion has received more attention lately (*1, 2*), but considerable difficulty is involved in measuring motion in many biological situations where one must avoid loading the structure being examined. Only recently have instruments capable of such measurement become available. The techniques used have included Mössbauer systems, laser interferometry, laser holography, capacitive probe, and modulation of reflected light (*3*).

As part of a study of insect sounds, I became interested in measuring the sound-radiating motion of the exoskeleton of intact and relatively unrestrained insects. Markl (*4*), through a consideration of the mechanics of the file and scraper system used by many stridulating insects, predicted the possible waveform of cuticular motion, but to my knowledge no one has observed this motion owing to inherent limitations of the available techniques. Described here is a simple method capable of making these measurements on hand-held insects. The technique involves sensing movement-induced light modulation over a small area of the insect's surface. Incorporated into the instrument is a continuous calibration of the output signal. The technique can be applied to many situations where vibration or position must be monitored, for instance in seismometry or barometry (*5*), but it is especially useful when noncontact measurement is desirable. Possible biological applications include measurement of substrate-borne sound, spider web vibration, water surface motion, and tympanic membrane motion (*2*).

Figure 1a shows a diagrammatic view of the motion-sensing elements of the measuring instrument. The target surface, normally the cuticle of an insect, is illuminated from the right of the figure by a high-intensity light beam. An opaque shield, made from a section of razor blade, partially occludes the light beam and casts a shadow on the target. When the target is properly positioned some of the light passing the shield strikes the target surface and is reflected through a narrow tube to the light detector, a miniature PIN (positive-intrinsic-negative) photodiode, whose output current is a linear function of irradiance (*6*). The narrow tube acts as a light guide serving to

0036-8075/79/0105-0057$00.50/0 Copyright © 1978 AAAS

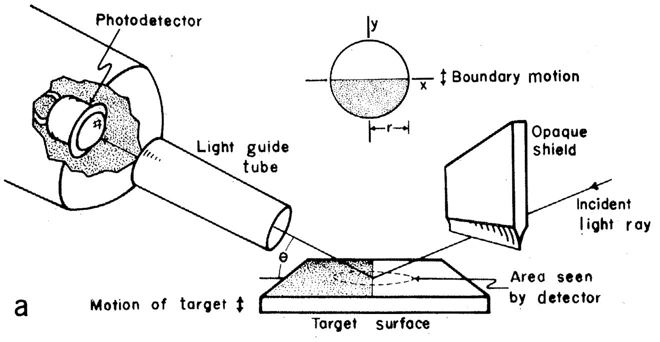

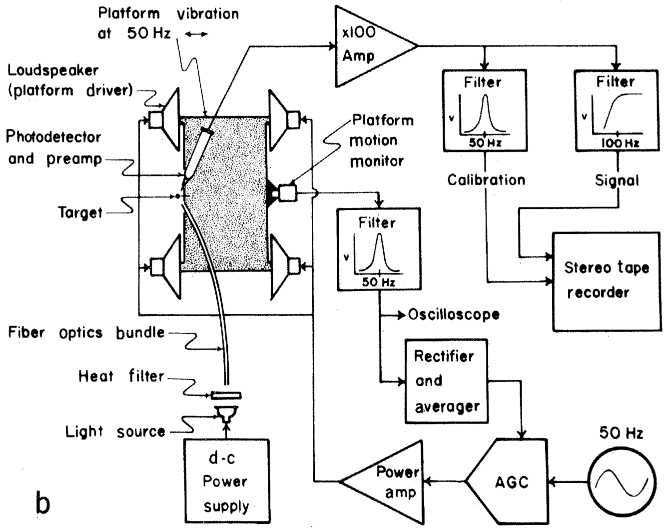

Fig. 1. (a) Motion-detecting components of the system, not to scale. Inset shows the target surface as seen through the light guide tube by the photodetector (miniature PIN photodiode HP 5082-4205). For the configuration of the apparatus described, $r = 125\ \mu m$ and $\theta = 23°$. (b) Platform motion control, light source, and signal recording system.

restrict the area viewed by the photodetector. The inset in Fig. 1a shows the target surface from the point of view of the photodetector looking down the light guide tube. Let us assume for now that the average position of the shadow boundary on the axes of the inset is at $y = 0$, the position of maximum sensitivity to motion. When the target moves slightly upward in Fig. 1a, more of the area seen by the photodector becomes shadowed by the opaque shield and the shadow boundary shown in the inset moves in a positive direction along the y-axis. This causes the lighted area seen by the photodetector to decrease and, as a consequence of this drop in illumination, the output of the photodetector to drop. Conversely, when the target surface moves slightly downward, the output of the photodetector increases. For small motions of the target, the photodetector output is a linear function of target motion.

The maximum displacement of the target surface which can be transduced by the instrument without significant distortion depends on r, the radius of the light guide tube, and θ, the angle between the target surface and the light guide tube which is set to equal the angle of incidence of the light beam. A vertical displacement m of the target surface causes the shadow boundary to move along the y-axis of the inset by $2m\cos\theta$. As long as this quantity is $<< r$, the change in illuminated area caused by such a motion is very nearly $2r(2m\cos\theta)$. Photodetector output is proportional to the illuminated area seen through the light guide. Since the change in illuminated area is linearly related to m for small motions (r and θ are constants), the output signal of the photodetector is also a linear function of the target motion.

When the displacement m becomes larger, the change in illuminated area departs from linearity because the aperture of the light guide is circular. The exact equation for the change in illuminated area $a(t)$ of the aperture as a function of time is

$$a(t) = 2\int_{y_0}^{y(t)} (r^2 - y^2)^{1/2} dy$$

where $y(t) = y_0 + m(t)\ (2\cos\theta)$ gives the shadow boundary motion about the average position of the shadow boundary y_0 for time-dependent motion $m(t)$ of the target surface (*7*). The signal output is proportional to $a(t)$ if the target surface is homogeneous and uniformly illuminated. When target motion is sinusoidal and $y_0 = 0$, calculation of the first six coefficients of the Fourier transform of the output equation for different amplitudes of target motion indicates that total harmonic distortion (THD) does not exceed 1 percent for motion of the shadow boundary $< 0.4\ r$ (*8*). For the particular configuration of the apparatus used, $r = 125\ \mu m$ and $\theta = 23°$. Therefore, amplitudes of motion up to $\sim 30\ \mu m$ can be measured without significant distortion. The minimum detectable displacement depends on several factors (*9*), but measurements of motions on the order of 0.1 nm have been made. The instrument thus has a dynamic range of > 100 dB.

In the preceding discussion I assumed that the average position of the shadow boundary y_0 is at $y_0 = 0$, which is to say that the average position exactly bisects the area seen by the detector. There are two undesirable consequences to shifting the shadow boundary away from this optimal position. First, THD increases because of the circularity of the light guide aperture. When $y_0 = 0.5\ r$ for example, THD is calculated to reach 1 percent at an amplitude of target motion of $\sim 3\ \mu m$ [see (*8*)]. The second undesirable effect is a decrease in the sensitivity of the apparatus because a given displacement m of the target surface produces a smaller change in illuminated area as y_0 moves away from $y = 0$. However, if this unwanted background motion of the target is such that the average position of the shadow boundary remains in the range $y_0 = \pm\ 0.6\ r$, the instrument is relatively insensitive to the position of the shadow boundary. Within this range the output for a given small displacement m changes by only ± 1 dB.

Nevertheless, position-dependent change in sensitivity can be especially bothersome when the target is a struggling, hand-held insect. Furthermore, sensitivity also depends on the reflective properties of the cuticle itself—shiny cuticle produces a larger output signal than dull cuticle for a given motion [see (*9*)]. Both these considerations necessitate a method for constantly monitoring instantaneous sensitivity. This is achieved by introducing a reference signal corresponding to a known vibratory amplitude into the output signal of the photodetector. Since the photodetector cannot distinguish between its own motion and that of the target surface, the motion-sensing elements can be mounted on a rigid platform which is driven sinusoidally at a known amplitude. The output of the photodetector will then consist of the signal due to target motion superimposed on the signal due to platform motion. If the calibration frequency lies outside the signal band of interest, it can be isolated by filtering and its amplitude compared with that of the signal produced simultaneously by motion of the target surface to gain an absolute measure of the vibrational amplitude of the target.

Figure 1b shows the system for providing such a reference motion and for recording the target motion signal and calibration. The platform on which the detecting apparatus is mounted is driven at a frequency of 50 Hz by direct attachment to the drivers of four loudspeakers. A calibrated detector, the platform monitor (*10*), constantly senses platform position. The output of the platform monitor is band-pass filtered and observed on an oscilloscope in order to set the amplitude of platform motion. The output of the monitor is also rectified and averaged to produce a d-c voltage proportional to the amplitude of platform motion. This d-c voltage controls the gain of an automatic gain control (AGC) which sets the amplitude of the 50-Hz driving voltage to the platform. The AGC permits platform motion to be stabilized at any amplitude between 1 and 10 μm peak, and if the platform is accidentally bumped during a recording session the AGC rapidly restores platform motion to its former level. The light source is a high-intensity, quartz-halide bulb powered by a d-c supply in order to avoid fluctuation in light intensity which would be produced by 60-Hz line current. The light passes through a heat filter and then via a 3-mm diameter noncoherent fiber optics bundle to the platform where it illuminates the target. The miniature PIN photodiode detector is positioned inside a 26-gauge hypodermic needle which functions as the light guide tube. To avoid attenuation of high frequencies in the output signal, the photodiode is immediately followed by a unity gain preamplifier having low input capacitance, high input impedance, and low output impedance. The preamplifier output is amplified by a factor of 100 and then filtered, in parallel, by a 50-Hz band-pass filter which gives the calibration signal, and a high-pass filter with sharp low-frequency roll-off which gives the target motion signal above 100 Hz. These two signals are recorded simultaneously on a stereotape recorder (*11*).

An example of the use of the apparatus to record vibration during sound production by a longhorn beetle (*12*) is shown in Fig. 2. This beetle produces sound using a file and scraper mechanism located in the middle of its back at the juncture of the wing covers and thorax. Markl (*4*) predicted that the vibration pattern of such a file and scraper arrangement should consist of a sawtooth waveform because of movement of the scraper over the transverse ridges (the teeth) of the file, with an impulse waveform superimposed each time the scraper strikes a tooth. Figure 2, trace a, shows a burst of vibration produced by a single pass of the scraper across the file. The expanded waveform (trace c) shows the roughly triangular form that Markl predicted, but tooth-strike impulses are not prominent. A sonagram (Fig. 2f) of the cuticular motion in trace a shows the harmonic series one would expect for a sawtooth waveform, but none of the broadband energy expected from an impulse. Nevertheless, such impulses are present and are seen in the airborne sound shown in trace d, which was produced by the vibration in trace a. Here impulses coinciding with each tooth strike are clearly evident, and a sonagram (Fig. 2g) of a portion of this sound shows the expected broadband energy of an impulse. Why are such impulses not evident in the recordings made of the cuticular vibration? Calculation of the motion necessary to produce the sound in trace d gives an approximate cuticular motion of 20 nm peak to peak (*13*). This motion is much less than the ~ 1 μm peak-to-peak motion of the cuticle shown in trace c and in fact lies below the background noise level of the recordings (*14*). The explanation for the disparity, evident in the sonagrams, between airborne and vibrational spectral energy distributions lies in a consideration of the radiation efficiency of the insect (*15*). This spectral noncorrespondence illustrates a general problem, namely that merely knowing the output of a microphone picking up airborne sound usually does not permit one to reconstruct the underlying vibration giving rise to the sound.

It was precisely this difficulty that prompted development of the vibration-sensing instrument described here. The original motivation for measuring cuticular motion was provided by behavioral tests of the effect of insect "disturbance" sounds (*16*) on spiders, animals well-known to be sensitive to vibration

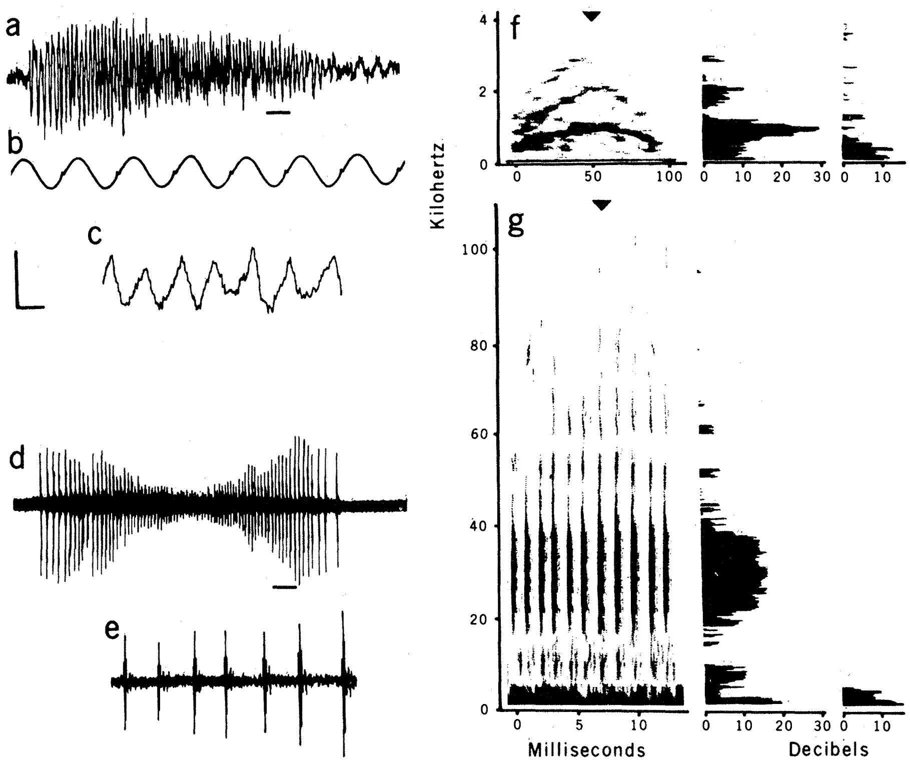

Fig. 2. Trace a shows vibration (150 to 15,000 Hz), recorded from the middle of one wing cover, produced by a sweep of the scraper across the file. For recording, the beetle was grasped with fingers by its legs and positioned while being viewed through a low-power dissecting microscope at the point labeled *target* in Fig. 1b. Optimal positioning was maintained by monitoring the 50-Hz calibration signal with headphones. Trace b shows the 50-Hz calibration signal recorded simultaneously with (a). In (b) the small pulse on the positive slope indicates the direction of outward motion of the cuticle and was introduced electronically just prior to recording. Trace c is an expansion of the underlined portion of (a). Trace d shows airborne sound (1 to 100 kHz) produced by the vibration in (a). Trace e is an expansion of the underlined portion of (d) and corresponds to the expanded vibration waveform in (c). The vertical calibration bar shows 1-μm movement in (a) and (c) (background noise ~0.08 μm_{rms} in these two traces); horizontal calibration is 10 msec for (a), (b), and (d) and 1 msec for (c) and (e). A sonagram (Kay Electric 7029A) of (a) is shown in (f) along with the spectral energy distribution (a section) taken through the region marked by a triangle and, at the far right, a section taken through background noise. A sonagram of (e) (plus four subsequent tooth strikes) is shown in (g) along with a section through the tooth strike marked by a triangle and a section through background noise. The analyzing filter bandwidth in (f) was 90 Hz. The effective bandwidth in (g) since the tape was analyzed at one-eighth speed [see (*11*)], was 4.8 kHz for the sonagram and 720 Hz for the sections.

(*17*). The resulting instrument, however, appears to have broad application in the measurement of small motions since it uses a noncontact, optical method having high sensitivity, good spatial resolution, broad bandwidth, wide dynamic range, and high tolerance of background displacements of the target surface (*18*). Furthermore, in contrast to many vibration detectors, it is relatively simple to construct, portable, easy to operate, and inexpensive. In order to adapt the instrument to other uses, only slight changes (*18*) are required to maximize sensitivity, bandwidth, spatial resolution, or background movement rejection at the expense of one or more of the others.

W. MITCHELL MASTERS
Section of Neurobiology and Behavior,
Cornell University,
Ithaca, New York 14853

References and Notes

1. B. M. Johnstone and A. J. F. Boyle, *Science* **158**, 389 (1967); J. Tonndorf and S. M. Khanna, *J. Acoust. Soc. Am.* **44**, 1546 (1968); A. Michelsen, *Z. Vgl. Physiol.* **71**, 63 (1971); J. A. Paton, R. R. Capranica, P. R. Dragsten, W. W. Webb, *J. Comp. Physiol.* **119**, 221 (1977).
2. H. Markl, *Z. Vgl. Physiol.* **57**, 299 (1967); V. A. Tucker, *Science* **166**, 897 (1969); R. S. Wilcox, *J. Comp. Physiol.* **80**, 255 (1972); K. Wiese, *ibid.* **92**, 317 (1974); A. Finck, G. M. Stewart, C. F. Reed, *J. Acoust. Soc. Am.* **57**, 753 (1975); P. H. Brownell, *Science* **197**, 479 (1977); A. J. M. Moffat and R. R. Capranica, *J. Acoust. Soc. Am.* **62**, S85 (1977).
3. P. B. Brown, B. W. Maxfield, H. Moraff, *Electronics for Neurobiologists* (MIT Press, Cambridge, Mass., 1973), pp. 315–317; P. R. Dragsten, W. W. Webb, J. A. Paton, R. R. Capranica, *Science* **185**, 55 (1974); *J. Acoust. Soc. Am.* **60**, 665 (1976); B. C. Hill, E. D. Schubert, M. A. Nokes, R. P. Michelson, *Science* **196**, 426 (1977); review by J. Tonndorf, *Acta Otolaryngol.* **83**, 113 (1977).
4. H. Markl, *Z. Vgl. Physiol.* **60**, 103 (1968).
5. For example, by using this technique to measure the displacement of a thin, aluminized Mylar diaphragm stretched over an enclosed air volume, a d-c coupled microphone or a sensitive barometer could be made. Such an instrument would not be limited at low frequencies by diaphragm capacitance as would be a conventional condenser microphone.
6. Photodiode output current is proportional to total power (watts) incident on the photodiode. Since the illuminated area of the photodiode is constant, output current is proportional to irradiance, or power per unit area.
7. The integral is the formula for the area of a circle between two lines drawn perpendicular to the circle's diameter.
8. When the detector was set up in its most sensitive position with the shadow boundary at $y_0 = 0$, accurate measurement of THD was impossible because of the difficulty of producing a target motion signal with less distortion than the detecting instrument. However, as the shadow boundary was shifted away from $y_0 = 0$, detector distortion increased and measurement of THD was possible. The THD measured by a spectrum analyzer (Nicolet Scientific, Miniubiquitous 444A) was less than predicted. There are two reasons for this, both a result of simplification of the theory of operation to permit easier understanding and analysis. First, the shadow boundary is not sufficiently sharp because the light source is not a point. Second, some light from outside the area seen through the aperture of the light guide reaches the photodiode via internal reflections in the light guide tube. These two factors moderate the distortion-producing edge effects by making changes in illumination of the photodiode more gradual than predicted.
9. The minimum detectable motion of the target surface depends on both the reflective properties of the surface and on the signal bandwidth. If the target is diffusely scattering rather than specular, much of the light striking the target is scattered off beyond the admittance angle of the light guide and, therefore, a given change in illuminated area produces less change in irradiance of the photodetector and hence less change in output. Signal bandwidth is also a major consideration since background noise is proportional to bandwidth. Over the full motion-bandpass of the instrument (10 to 120,000 Hz) the equivalent input noise motion (that is, the target motion that would produce the measured output noise if the detector and preamplifier were noiseless) is 0.043 μm_{rms} (where rms is root mean square) for a specular target (front-surface mirror) and 0.7 μm_{rms} for a scattering target (white, nonglossy paper). For insect cuticle, the equivalent input noise motion will depend on the properties of the cuticle but will normally lie between these values. Reflectivity of an insect's surface can be increased by attaching a small piece of aluminized Mylar tape to the insect. Under optimal conditions (specular target) amplitudes of motion on the order of 0.1 nm have been measured, at a signal-to-noise ratio of ~ 10 dB, by means of lock-in detection with an effective analysis bandwidth of 0.01 Hz.
10. P. B. Brown, *IEEE Trans. Biomed. Eng.* **21**, 428 (1974). The sensitivity of this detector, as determined by static displacement of the platform with a micrometer, was 21.6 mV/μm.
11. Since the upper frequency limit of the stereo tape recorder (Uher 4400 Report Stereo IC) is approximately 15 kHz (± 1.5 dB from 50 to 15,000 Hz) and insect sounds frequently extend to ultrasonic frequencies, the signal is also recorded on an instrumentation tape recorder (Lockheed 417, not shown in Fig. 1b), which has a frequency response extending to 100 kHz (± 1 dB from 1 to 100 kHz when recorded at 76 cm/sec and replayed at 9.5 cm/sec for analysis). The airborne sound associated with the vibration signal being studied is also recorded on the instrumentation recorder by means of an ultrasonic microphone (± 1.5 dB from 1 to 100 kHz).
12. *Enaphalodes rufulus* (Cerambycidae).
13. Each pulse in Fig. 2, trace d, consists of several cycles of damped oscillation at about 30 kHz. A 30-kHz sine wave having the maximum amplitude of any pulse in trace d would have a sound pressure at the microphone of approximately 75 dB sound pressure level, which corresponds to a peak-to-peak amplitude of molecular air motion of about 4 nm. Since the sound was recorded at a distance of 38 mm and the beetle can be approximated as a radially pulsating cylinder 7 mm in diameter, an impulsive motion of the cuticle of ~ 20 nm would be necessary to produce the airborne impulse.
14. Amplitudes of motion on this order can be measured with this instrument by using signal processing techniques such as lock-in detection, signal averaging, or autocorrelation, but these techniques are infeasible when applied to insect disturbance sounds due to the broadband, transient and unpredictable nature of these sounds.
15. Radiation efficiency is low when the dimensions of the vibrating source are small compared to the wavelength of the radiated sound [see P. M. Morse, *Vibration and Sound* (McGraw-Hill, New York, 1948)]. Thus, although the maximum energy of vibration is at about 1 kHz in Fig. 2, trace a, little sound is radiated at this frequency because the beetle is only ~ 7 mm wide compared to a 1-kHz wavelength in air of ~ 340 mm. On the other hand, the frequency of maximum airborne enrgy is at about 30 kHz. At this frequency the wavelength in air is ~ 11 mm and so coupling of vibration energy to air is more efficient.
16. Many different insects produce sounds when handled or otherwise disturbed. It has been proposed that these disturbance sounds serve to startle or warn potential predators [P. T. Haskell, *Insect Sounds* (Quadrangle Books, Chicago, 1961); T. Eisner, D. Aneshansley, M. Eisner, R. Rutowski, B. Chong, J. Meinwald, *Psyche* **81**, 189 (1974); T. Bauer, *Z. Tierpsychol.* **42**, 57 (1976)].
17. C. Walcott, *Am. Zool.* **9**, 133 (1969); A. Finck, *ibid.* **12**, 539 (1972).
18. Specifications depend on the configuration chosen and on the associated electronics. A more complete description of the apparatus will be published elsewhere (W. M. Masters, in preparation). For the instrument described here, maximum sensitivity to motion is 134 mV/μm with a broadband noise of 5.8 mV_{rms}, the target area seen is ~ 0.14 mm^2, the 3-dB motion-band pass is 10 to 120,000 Hz, the dynamic range is > 100 dB, and background motion of the target can be up to 80 μm for < ± 1-dB change in output.
19. Supported in part by an NSF predoctoral fellowship and a Bache Fund stipend (to W.M.M.), and NIH grant AI-02908 and NSF grant BMS 76-15084 (T. Eisner). The insects were identified by E. R. Hoebeke and the insect identification service of the U.S. Department of Agriculture. I thank the director and staff of the Archbold Biological Station, Lake Placid. Fla., where the recordings of insect sounds were made, R. R. Capranica for the loan of various pieces of electronic equipment, and D. Aneshansley, R. R. Capranica, T. Eisner, and A. J. M. Moffat for their comments on the manuscript.

18 April 1978; revised 17 July 1978

Synaptic Phosphoproteins: Specific Changes After Repetitive Stimulation of the Hippocampal Slice

Abstract. *Repetitive stimulation (100 pulses per second for 1 second) of the Schaffer collateral-commissural system of the rat hippocampus induces long-term potentiation of synaptic strength and produces significant changes in the subsequent endogenous phosphorylation of a 40,000-dalton protein from synaptic plasma membranes. This effect is not observed after stimulation in calcium-deficient media or after simulation at the rate of one pulse per second for 100 seconds. These findings provide evidence that repetitive synaptic activation can alter the phosphorylation machinery of the synaptic region and suggest a biochemical process which may be involved in the production of neuronal plasticity.*

Historically, synaptic transmission has been analyzed in terms of biochemical and physiological events that take milliseconds to transpire. Recently it has become evident that, under some circumstances, the efficacy of the transmission process can be modified for periods ranging from minutes to months (*1*). There is evidence that phosphoproteins may be involved in such synaptic events. Protein phosphorylation can occur within seconds and is known to persist for at least minutes (*2*); this alone makes the process attractive as a candidate for the biochemical substrate of relatively long-lasting changes in synaptic efficacy. Furthermore, a number of studies have provided evidence linking the phosphorylation machinery to synaptic events. Protein kinases, protein phosphatases, and their substrates have all been found in fractions enriched in synaptic plasma membranes (SPM's) (*3*). Other studies have shown that electrophysiological